HYBRID CONSTANT DIRECTIVITY HORN

Presented by Dario Cinanni at the Audio Engineering Society 148th Online Convention 2020 June 2-5

ABSTRACT

A new horns family is presented, the Hybrid Constant Directivity (HCD), investigating some practical aspects of constant directivity design through physical and FEA 3D prototypes. Horn driver SPL simulations are conducted using a method already presented to the scientific community and here improved, lead to a minimum mismatch between horn simulations and measurements. A detailed directivity and numerical match of the beam-width are examined with a direct SPL comparison among exponential, tractrix and spherical expansions. Then, horns aspect ratio is changed obtaining HCD elliptical and rectangular mouth horns referenced and correlated to the circular one SPL simulation. Also wave-front shapes, mouth diffraction effects and radiation impedances are analyzed. Finally, the mathematical model for calculating HCD horns is disclosed.

1 Background

This article has been written starting from an acoustic simulation study presented at the *Comsol 2015 Conference*, Grenoble (France) [1]. On that research a new simulation method, about high frequency horn driver transducers, was presented. The method comprises a horn simulation and a compression driver plane wave tube (PWT) measurement. Combining only these two data, using a novel equation that correlates the matrix of the virtual horn and the physical compression driver pressure, is possible to easily predict the absolute sound pressure level of the real horn driver frequency response. The following equation has been presented:

$$L_{pt_{f_x}} = 10\log_{10}\left[10\,\hat{}\left(\frac{L_{pPWT_f}}{20}\right)\cdot p_{sim_{f_x}}\right]^2 + \left(L_{pPWT_{fx}} - L_{pPWT_f}\right)$$

Where $L_{pt_{f_x}}$ is the horn driver absolute sound pressure level calculated for each frequency, L_{pPWT_f} is the compression driver sound pressure level measured on PWT at a given frequency, $p_{sim_{f_x}}$ is the sound pressure of the horn simulation calculated for each frequency and $L_{pPWT_{fx}}$is the compression driver sound pressure level measured on PWT for each frequency. L_p are expressed in dB and p in Pa. The results showed a good match between simulations and measurements up to 15 kHz. We found that the main limit is the assumption of a plane wave, which does not hold for higher frequencies. On section 4 is described the improved model.

2 Hybrid Constant Directivity (HCD)

The two main reasons why horns are used in sound systems are high efficiency (and consequently high SPL at relative low distortion) and directivity control. We want to focus on the second point: directivity. The question is: is it possible to transform a conventional expansion horn (exponential, hyperbolic sine, hyperbolic cosine, catenoidal, tractrix, spherical, etc.) into a constant directivity horn, without loose sound characteristics of the expansion? Considering a mathematical expansion law of a horn it is possible to extend expansion profiles for a progressive match between throat and different mouth shapes. If we keep the defined horn expansion law following the same volume expansion, within certain limits, we can modify boundary profiles to satisfy special needs. The necessity we want to satisfy is the constant directivity, maintaining the sound characteristic that identify the expansion. The horn mathematical progression is always guaranteed, so the key is to have a non-deformable volume gradient. In this way if we want a hyperbolic cosine profile we will maintain the same load and low frequency control, but we can obtain also the directivity control on one plane.

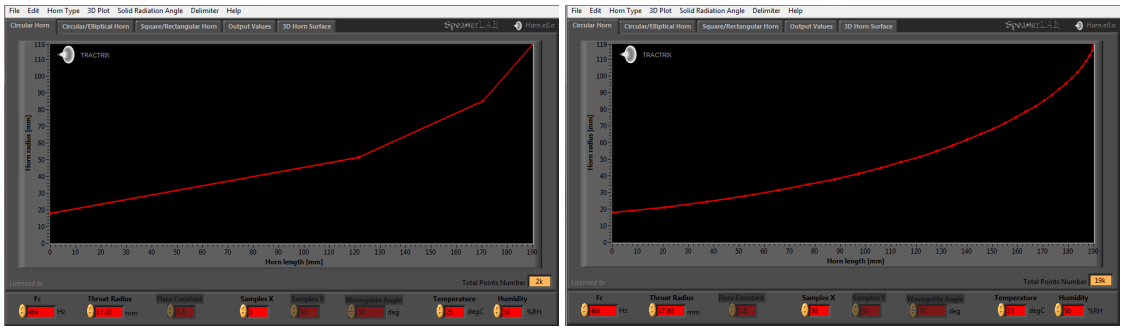

Figure 1. Sample X represents the segments number that approximates the horn volume expansion on the x axis. X=3 (left), X= 30 (right).

The volume expansion is discretized by the X, Y values number. As for the 2D mathematical profile, the 3D volume discretization approximates the selected ideal expansion. Better approximation occurs when reducing the step as it is observable in Fig. 1. For the current prototypes, on x axis for example, an X value is carefully selected to obtain a step of 1.85mm, thus every step the horn volume adapts its expansion matching the selected mathematical law. This is a coarse step, generating a 61k 3D point's cloud, useful for a demonstration purpose, but for an accurate surface reconstruction of a similar product with this dimension it's suggested a finer mesh, about 1M points. We can call these kinds of horns **Hybrid Constant Directivity** (**HCD**) and they can guarantee:

- the expansion we already know;
- a progressive constant directivity on the plane along its mouth major axis;
- an equivalent directivity contour of a circular mouth horn (using the same expansion) on the plane along its mouth minor axis.

With this type of horns the maintenance of constant directivity with frequency in high-frequency exponential horns (and all other expansions) is possible on one plane and the constant directivity progression depends on the mouth ratio. These kinds of horns are useful for all applications where a directivity control on one plane is requested. Various HCD horns are nowadays available on the market, mainly from the Italian professional audio manufacturer as single components and used all over the world in diverse loudspeaker systems, also for home hi-fi.

3 Aspect-Ratio

First of all we are going to analyze a commercial 1.4 Inch throat elliptical mouth horn (Fig. 2), which was calculated using *SpeakerLAB Horn.ell.a* [2].

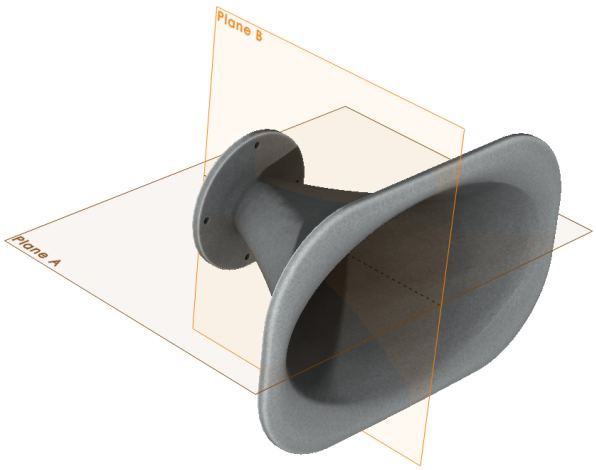

Figure 2. Section planes. Plane A along the major axis of the horn mouth and plane B along the minor axis.

We can use constant directivity along a vertical line or along a horizontal line; it depends on requirements and by the application. For this reason, to avoid confusion, I prefer to talk about general planes and not vertical or horizontal one. For convenience we define here two section planes. **A** is the section along the major axis of the horn mouth (the plane **A**

here is always referred to the constant directivity section plane) while **B** is the one along the minor axis. This is true when the horn mouth has an aspect-ratio>1. The **mouth aspect-ratio** (**MR**) is always referred to the horn mouth and it represents the ratio between mouth major and minor axis. Usually ratios between values of 1 and 1.8 are used. As we know, the directivity of a horn is controlled down to a frequency that has a wavelength comparable to the horn mouth. Regarding the two perpendicular section planes square mouth horns will have the same directivity at lower frequencies, so for a square horn it is possible to modify its directivity only in a limited frequency range. For this reason a square HCD horn is treated as a circular horn. If MR= 1 the horn has a circular or a square mouth and we have only one section plane (because plane A= plane B). It's possible to have MR> 2, maintaining the selected expansion and reducing wave-front deformations. Modifying the mouth ratio of a horn by means of the new mathematical model, it changes the major and the minor axis, gradually transforming the major axis in a pseudo-conical profile, obtaining a constant directivity on one plane. In the next sections we will see how it is possible to increase the aspect-ratio, discover how the aspect-ratio value is linked to the constant directivity coverage angle and why the aspect-ratio value is being increased.

4 Horn driver model

A rigid circular piston, with a planar surface and the same radius of the horn throat, has been modeled as a source to load all simulated horns. This condition produces an acoustic pressure, in order to predict horns directivity. The standard model generates directivity as seen in Figs 3, 4, analyzing these contours, starting from a certain frequency the simulated high frequency band is different compared to the final product measurements graphs (Figs 5, 6).

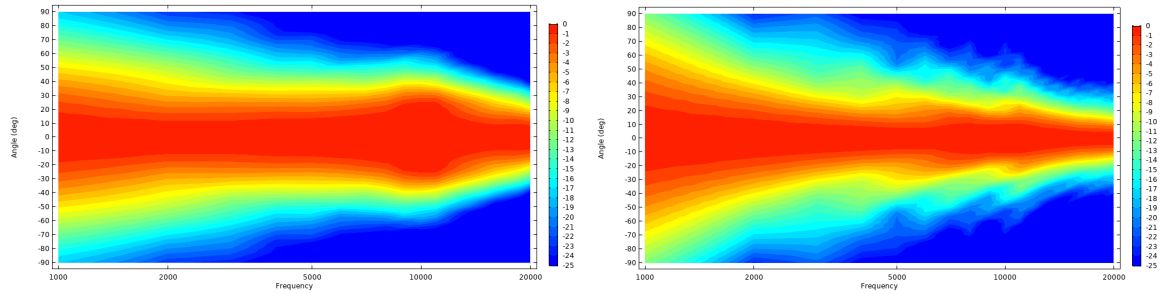

Figures 3, 4. Simulated plane A (left) and plane B (right) directivity plots.

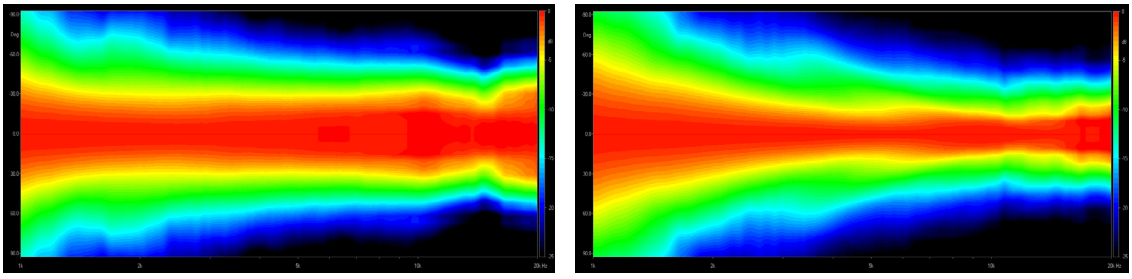

Figures 5, 6. Measured plane A (left) and plane B (right) directivity plots. Smooth 1/2 Octave.

The scope is trying to study in detail the horn driver high frequency directivity behavior, in order to improve simulations results and also to calibrate the model. This step is necessary if we want to predict horns directivity plots with a good accuracy.

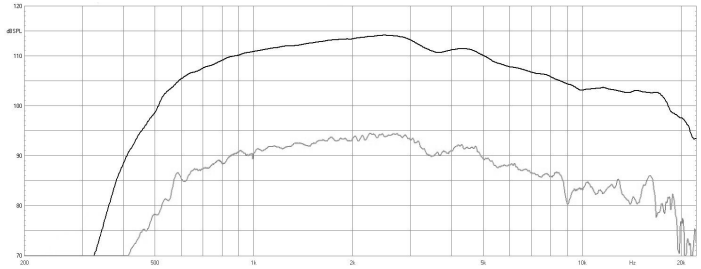

Figure 7. Horn driver 1W frequency response. Microphone on axis at 1m distance from the mouth. Measurement done in anechoic room in a free field condition. Upper curve smooth 1/3 Octave, lower curve -20 dB unsmoothed .

The measurements were done using a compression driver mounted to the physical horn as given in Fig. 2; together they produce a frequency response as Fig. 7 shows. If we put the compression driver phase-plug into the simulated model, we can see that simulations of Figs. 8, 9 and measurements of Figs. 5, 6 are very similar now, with an improved match at higher frequencies.

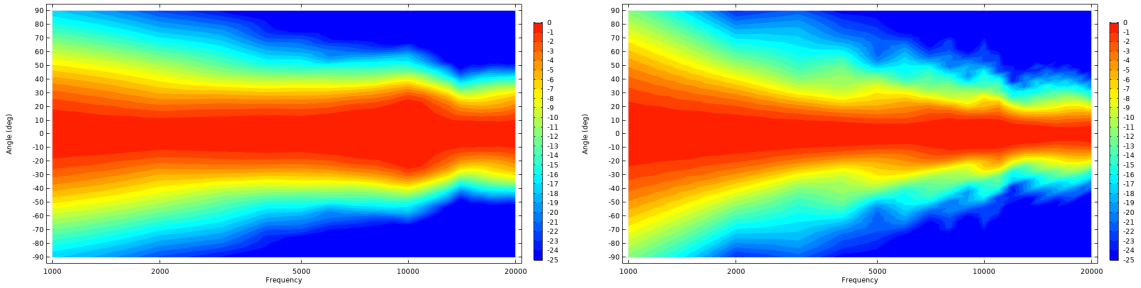

Figures 8, 9. Simulated plane A (left) and plane B (right) directivity plots. New horn model with the phase-plug added.

This is due to phase-plug acoustic expansion on its channels exit. Consequently, starting at a certain frequency, which depends on the horn throat diameter, the higher frequency directivity depends more on geometry, shape, channels number and mathematical progression of the phase-plug. Then a thermo-viscous acoustic is applied on the phase-plug channels adding losses for an improving result. To understand better why the main limit is the assumption of a plane wave on the horn throat it is

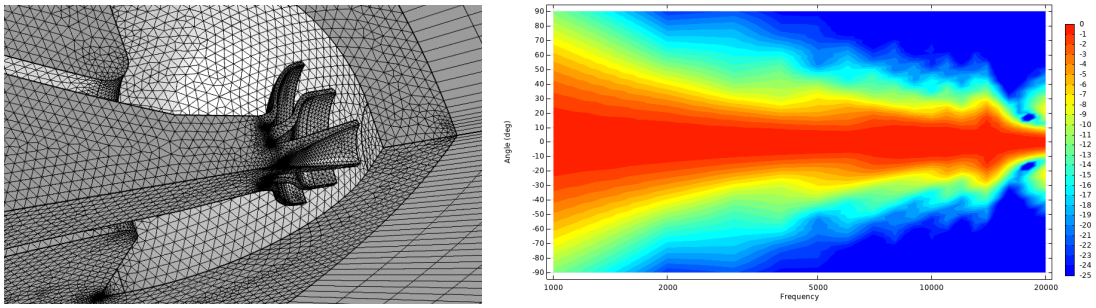

Figures 10, 11. One of the first phase-plug prototypes added to the used model, which produces the plane B directivity plot.

reported the behavior of one of the first phase-plug prototypes (Fig. 10) which produces a plane B directivity plot of Fig. 11. Examining the sound pressure distribution on the horn throat (Figs. 12, 13), we can see that on the boundary, generally modelled for the ideal plane wave, the wave-front arriving from the phase-plug is not uniform.

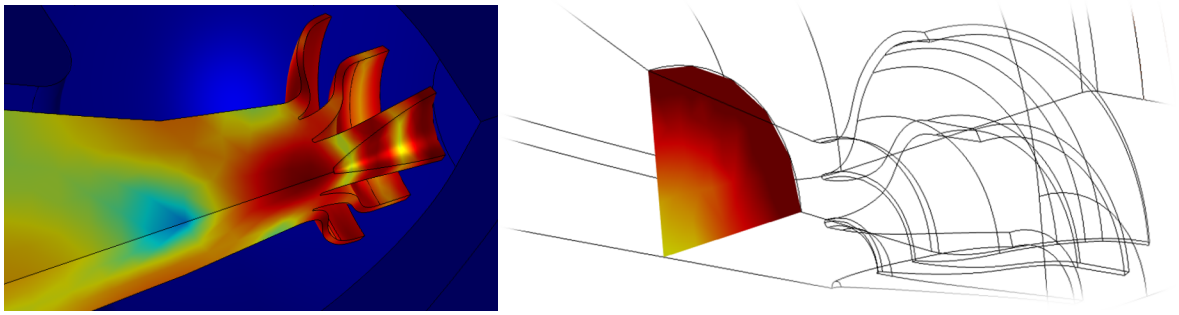

Figure 12. Horn throat sound pressure distribution @14 kHz.

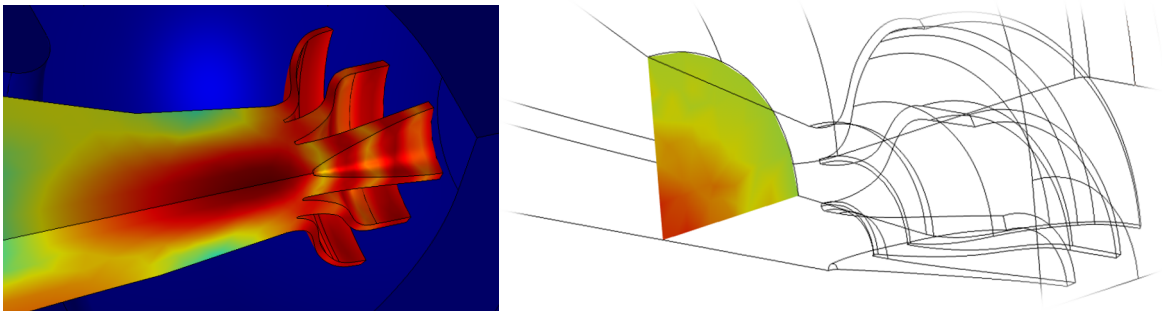

Figure 13. Horn throat sound pressure distribution @18 kHz.

Increasing the frequency the pressure transfers from the margins to the core of the horn throat. This is a clear and simple example that explains one of the phase-plug's aims, it has to align the wave arrival times trying to reproduce a plane wave on its exit and at the same time it has to suppress cavity resonances, using Bessel [3] functions (for the cylindrical cavity mode shape functions) or Legendre [4] functions (for the spherical cavity mode shape functions), for selecting phase-plug channels locations on nodal positions in the cavities, hence where they have the cavity mode shape functions (or Eigenfunctions) with a value equal to zero. As we know simulation accuracy is obtained when we model the full horn driver, with the entire compression driver comprising vibro-acoustic coupling for the membrane, because the systems are strongly coupled. However, simulating a virtual horn to combine it with a physical compression driver, with some smart ideas we can reduce the error to an acceptable level limiting the horn model to the acoustic path only, including the phase plug. Fig. 14 shows the final result of the simulation using the model described here and the method already presented on the introduction. My target is to have a general and valid horn model independent of the compression driver, because here I want to describe a new horn type, neither a driver nor a phase-plug.

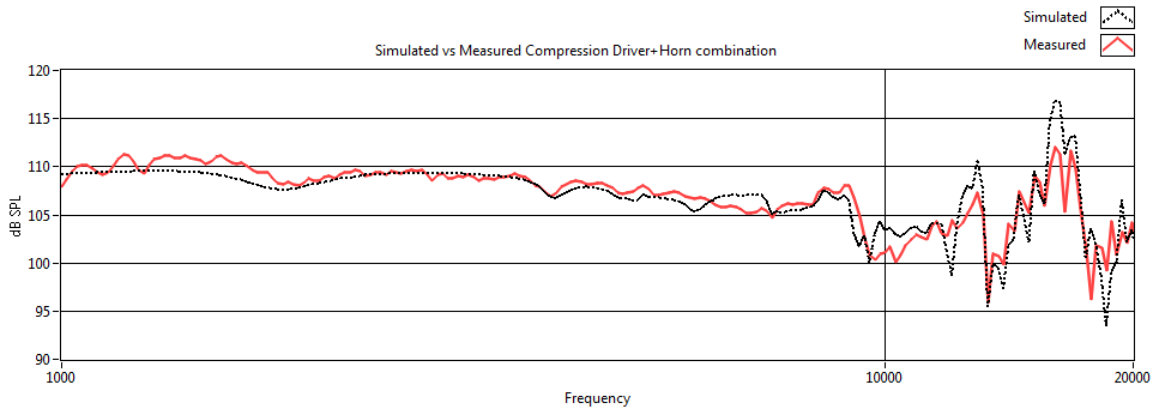

Figure 14. Measured (red) and simulated (black) 1÷20 kHz absolute sound pressure frequency response of a horn driver. The compression driver is a commercial 1.4 Inch available nowadays on the market. The horn is the same of Figure 2.

5 HCD horn directivity

Considering the chromatic match between simulations and measurements of the directivity color plots, in Figs. 15, 16 we can appreciate a numerical match of the beam-width. As generally defined, **beam-width** is defined here as the coverage angle in which an SPL loss of 6 dB occurs relative to the zero degrees reference angle (the on-axis direction). As we can see in the Fig. 15, on plane A the beam-width is well controlled, in this case we see a coverage angle of 62.3° in the frequency range 1.35÷20 kHz. On plane B (Fig. 16) from 4 kHz upward there is a regular beam-width, but it exceeds 6 dB, moreover it is not fixed but it depends on the selected expansion. So for the plane B we can calculate an averaged value but in my opinion it is not formally correct to give a unique value because the reader, or a buyer of a similar product, could be misled when comparing **HCD** to **CD** horns. This rule is valid also for all cases of horns with a non-constant directivity beam-width, for example all pure profiles as exponential, tractrix, spherical, etc. with a circular mouth. It doesn't make sense to declare a coverage angle with a single value in a similar situation, because, of course we can use them, but these horns in pure shapes were not thought for this purpose.

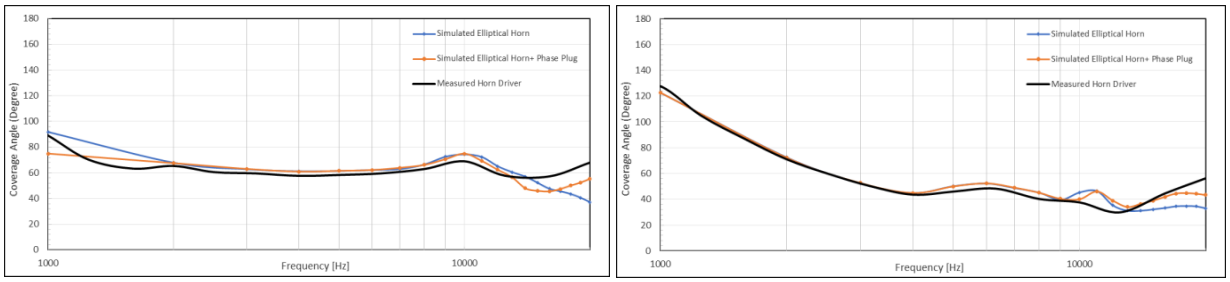

Figures 15, 16. Beam-width measurement and simulations on plane A (left) and plane B (right).

For HCD horns we can use for example the wording **COVERAGE ANGLE** x **SELECTED EXPANSION**, so Fig. 2 horn could be a commercial **62° x HYPERBOLIC**. For that reason I use the name "Hybrid" constant directivity horn. From the beam-width analysis we can see that it is possible to improve the model simply by adding a phase-plug. Anyway, up to 15 kHz the simplified model works well for our purposes, because you must always take into account that a different phase-plug (so a different compression driver) will influence the upper frequency range. Therefore, we can work with 3D horns simulations only -considering the model reliability- paying attention to all next directivity and beam-width plots and not considering the high frequency beam, because as we have previously seen in the real conditions for a 1.4 Inch horn directivity >15 kHz depends on the horn-driver combination.

6 Horn expansion efficiency

One of the most efficient horn expansions is the exponential profile. This horn is extraordinarily efficient as an acoustic transformer device due to its impedance match between the source of sound at the throat of the horn and the atmosphere into which the horn mouth radiates. But what is the SPL difference between an exponential expansion and other types?

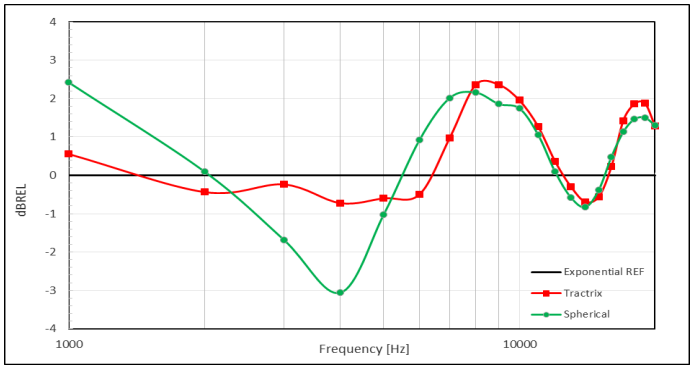

Figure 17. Exponential horn normalized frequency response (REF) and the relative difference of a tractrix (red) and a spherical (green) horn, referenced to the pure exponential one (black). Simulations @1m distance on axis.

Fig. 17 horns were designed starting from the same values. This interesting graph shows that near the cut-off frequency the tractrix and the spherical have more pressure. This is mainly due to the natural flared mouth of these expansions, compared to the pure exponential expansion whose calculus has an unflared mouth. Then there is a range in which exponential has more energy followed by a range in which tractrix and spherical have an averaged increased SPL. Starting from a pure exponential circular mouth profile, which produces directivity we already know for this standard horn type

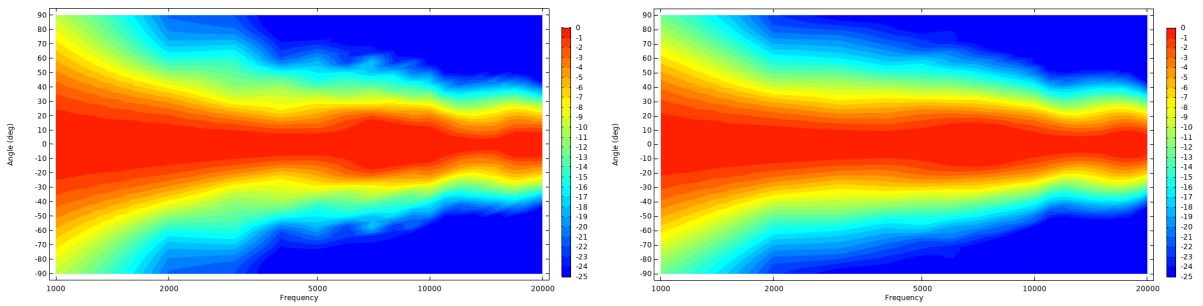

Figures 18, 19. Circular mouth pure exponential horn directivity (left), with flared mouth (right).

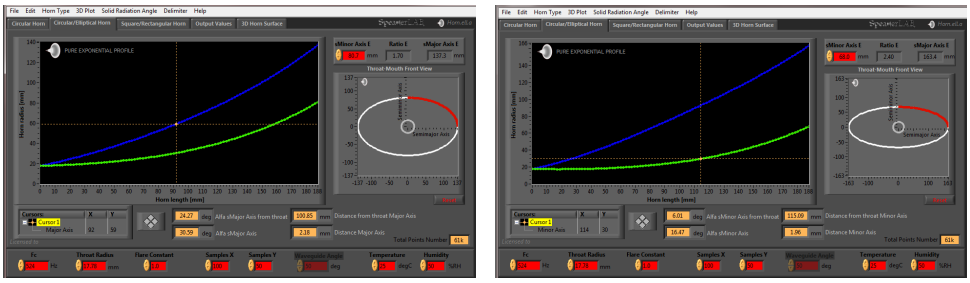

Figures 20, 21. Elliptical mouth HCD horns arrangement. MR= 1.7 (left), MR= 2.4 (right).

(Figs. 18, 19), we want to obtain two different horns simply acting on the minor axis value to increase mouth ratio, defining two HCD horns with two different ratios, MR= 1.7, MR= 2.4 (Figs. 20, 21). Directivity plots (plane A left and plane B right) of the two horns are reported in Figs. 22 to 29. Horns are in a pure exponential expansion with two different mouth ratios. It is shown also the directivity of the same horns with a flare added to the original design. We can read more about this point in section 8.

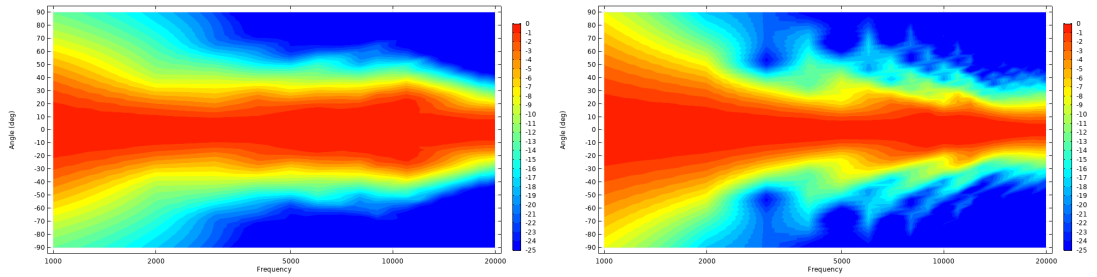

Figures 22, 23. Elliptical mouth HCD horn (MR= 1.7).

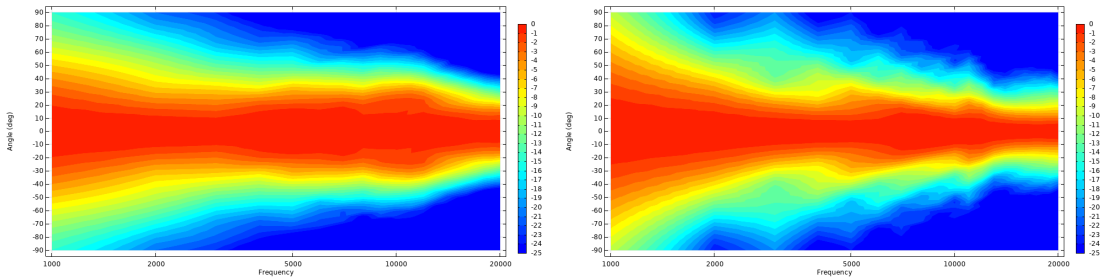

Figures 24, 25. Same horn of Figs. 22, 23 with flared mouth.

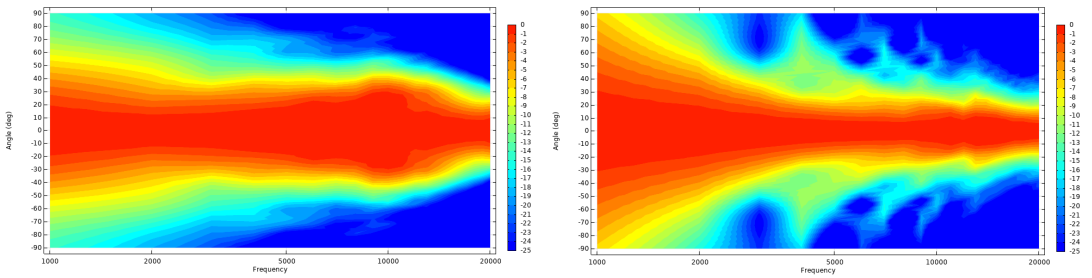

Figures 26, 27. Elliptical mouth HCD horn (MR= 2.4).

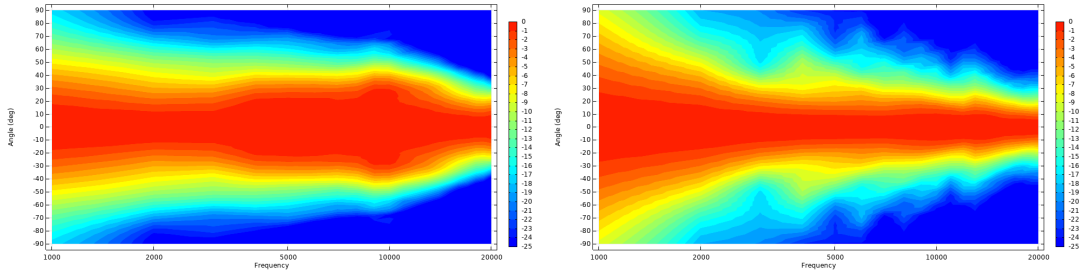

Figures 28, 29. Same horn of Figs. 26, 27 with flared mouth.

In Figs. 30, 31 we can compare simulated beam-width of the two elliptical horns. As we can see the two MR have a different constant coverage angle on the plane A, useful for a different application, respectively 65° (MR= 1.7) and 75° (MR= 2.4). Furthermore, when increasing MR we are also reducing the coverage angle maximum difference on the constant directivity plane (Fig. 30).

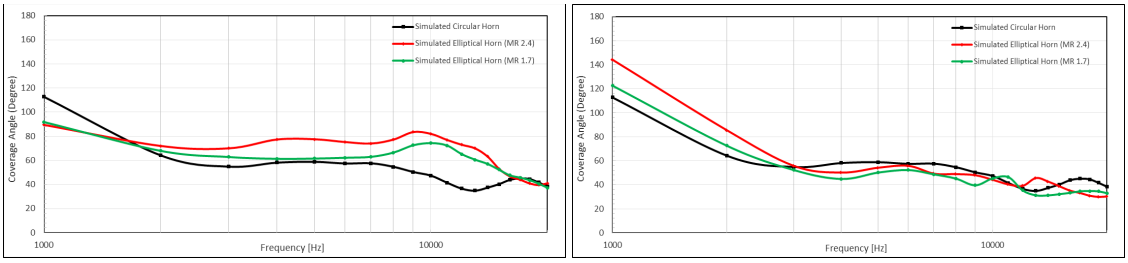

Figures 30, 31. Circular (black) and elliptical mouth horns beam-width comparison. HCD horn with MR= 2.4 (red) compared to the HCD horn with MR= 1.7 (green). Plane A (left) and plane B (right).

Analyzing the sound pressure between the circular horn and the elliptical one, we can see in Fig. 32 the relative SPL difference, simulated on axis at 1m distance. Obviously the circular has more energy because its beam-width is focused on axis, while elliptical ones have a spread energy around space because they cover a bigger angle on the plane A. It's interesting to see that the dB loss for the two elliptical horns is limited if compared to the circular one. The dB loss is controlled for a great portion of the frequency bandm, taking into account that for a rectangular mouth horn, analogous to the elliptical one with MR= 2.4, the relative on axis SPL difference is substantial.

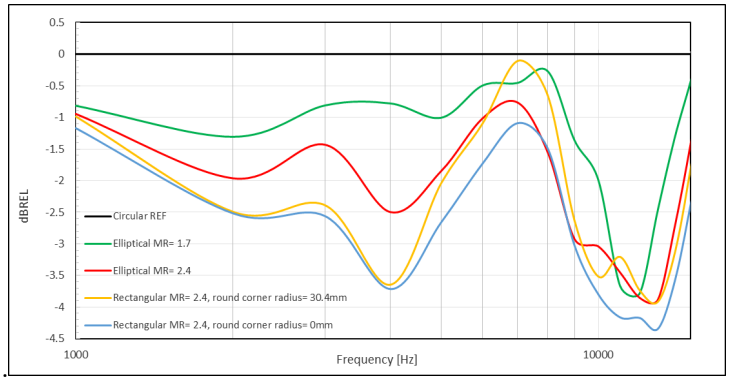

Figure 32. Normalized exponential circular (MR= 1 REF) horn frequency response and the relative SPL difference of the same horn expansion with modified mouth ratios.

Also, we can see that when increasing the MR value we increase a dB loss on-axis, because of an SPL off-axis on plane A intensification. Indeed, when simply moving the microphone 45° off-axis we can see in Fig. 33 the difference among the horns. The elliptical MR= 1.7 has more SPL on the great part of the frequency range compared to the others with MR= 2.4 referenced to the circular one. Then, fixing all parameters and adding a round corner radius (4 x 30.4mm) along its mouth we improve the SPL contribution of the rectangular mouth horn.

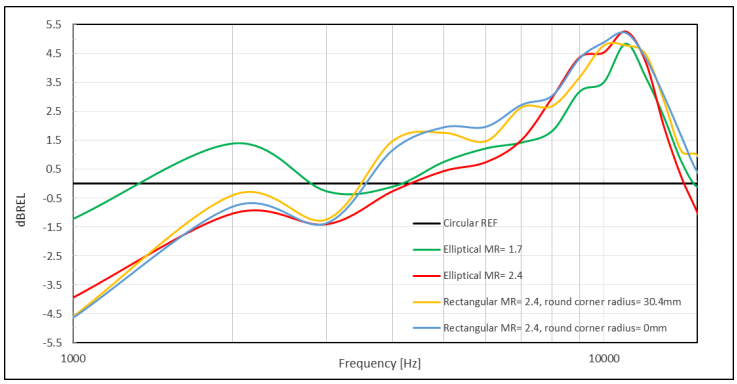

Figure 33. Same of Fig. 32 with mic. 45° off-axis on plane A.

Next images of Fig. 34 shows ¼ solid model of the before mentioned horns, with the relative surface mouth sound pressure level distribution plots for the center band frequency (10 kHz). As shown in Fig. 34d the rectangular horn, compared to the ellepical ones, suffers of the “corner effect”, which is because of reflections. For every frequency we will have a different behavior near the corner and it can influence the wave-front distortion and the general performance of the horn.

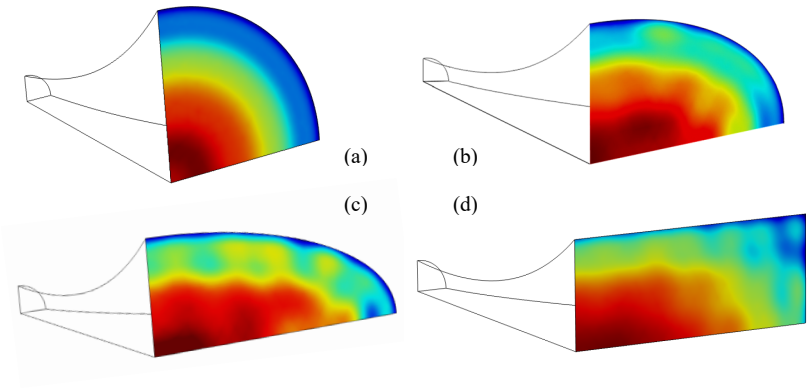

Figure 34. Horn mouth sound pressure distribution @10 kHz. Circular (a), elliptical MR= 1.7 (b), elliptical MR= 2.4 (c), rectangular MR= 2.4 (d).

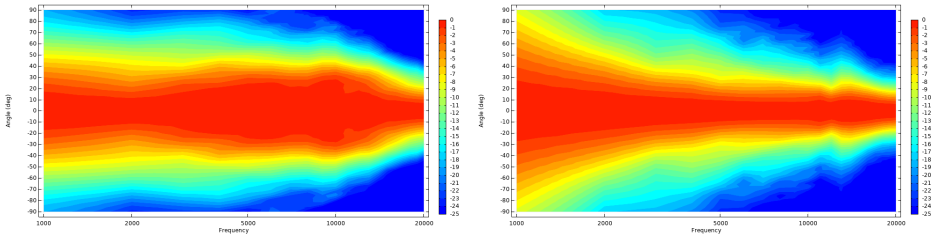

Figures 35, 36. Exponential HCD horn directivity of the round corner (30.4mm) rectangular flared mouth (MR= 2.4). Plane A (left), plane B (right).

This is a common problem of horns having rectangular mouths, while elliptical mouths horns avoid the lack of polar pattern control along the diagonal. Figs. 35, 36 are useful for a comparison with the other presented directivities.

7 Horn wave-front shape

Analogous to the coverage angle, the **coverage area** is defined as the area limited by the isobar having a level of 6 dB below the maximum value found on the sphere. The coverage area gives useful information about the horn wave-front shape. HCD horns generating a wave-front with a flat zone that has a contour similar to the horn mouth which generates it. In Figs. 37, 38, 39 are shown some examples of the wave-front shape @10 kHz of the examined HCD horns. The wave-front on the left and the particular of the coverage area on the right.

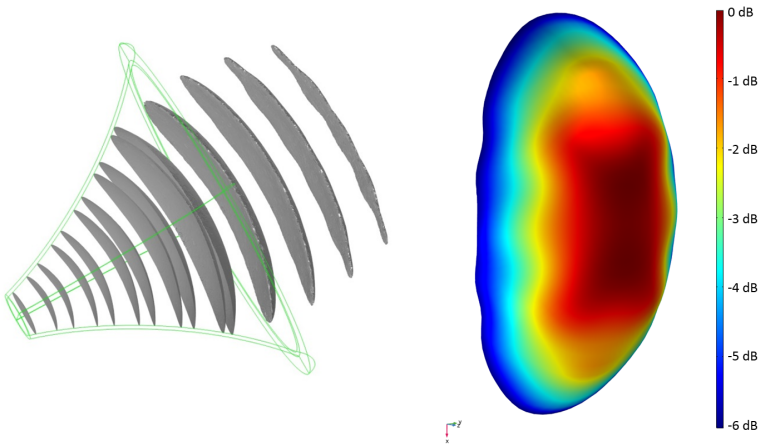

Figure 37. Elliptical flared mouth (MR= 1.7) exponential.

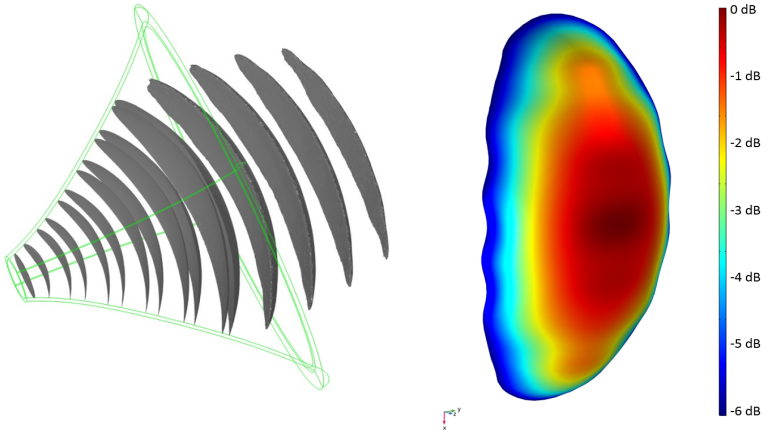

Figure 38. Elliptical flared mouth (MR= 2.4) exponential.

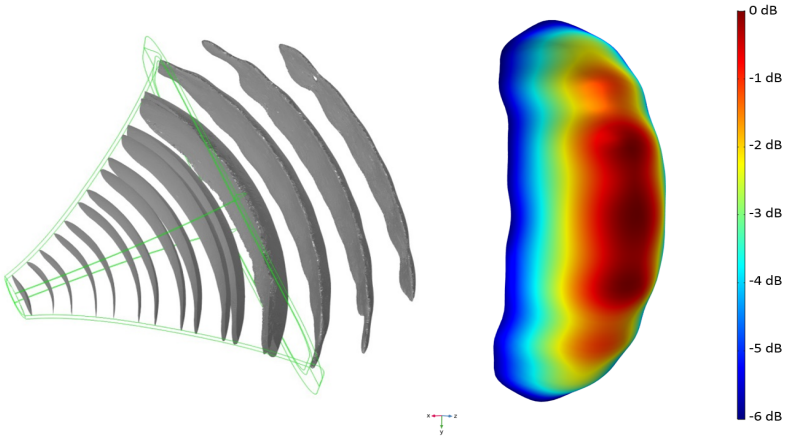

Figure 39. Round corner rectangular flared mouth (MR= 2.4) exponential.

8 Mouth diffraction effects

Some types of horns have a flared mouth (tractrix and spherical expansions for example), while the hypex family horns (exponential is included in this family) have an unflared mouth. It is reported the differences on the directivity polar patterns between a standard exponential horn compared to the same shape but with a flared mouth. From the graph of Fig. 41 we can see the frequency response deviation of the circular mouth exponential horn with a flared end loop of Fig. 40, along its mouth profile. Graph 42 shows the same comparison but related to the elliptical mouth exponential horn (MR= 2.4), using a similar flared end of Fig. 40. The flare shape is not optimized for a specific application and it is showed for the higher MR horn. Comparing Fig. 43 with 42, discrepancy may be explained by the influence of the cross-modes, clearly on elliptical and rectangular horns are not symmetrical.

Figure 40. Example of a flared end, solid part in red, added to the exponential expansions horn mouth profile.

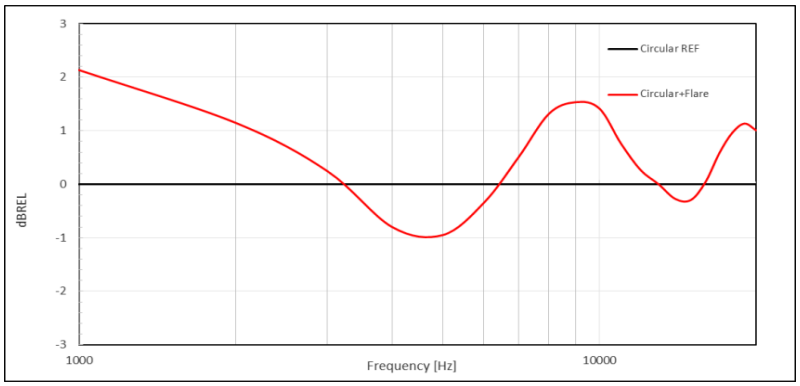

Figure 41. Normalized on axis frequency response of the circular mouth exponential horn with flared mouth (red), referenced to the same horn with unflared mouth (black).

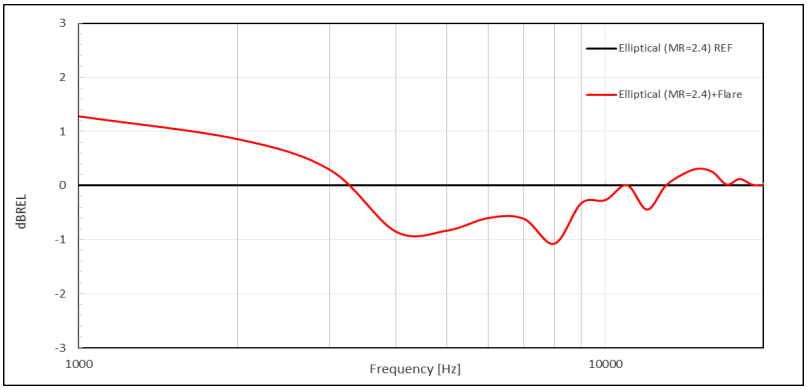

Figure 42. Normalized on axis frequency response of the elliptical mouth HCD exponential horn (MR= 2.4) with flared mouth (red), referenced to the same horn with unflared mouth (black).

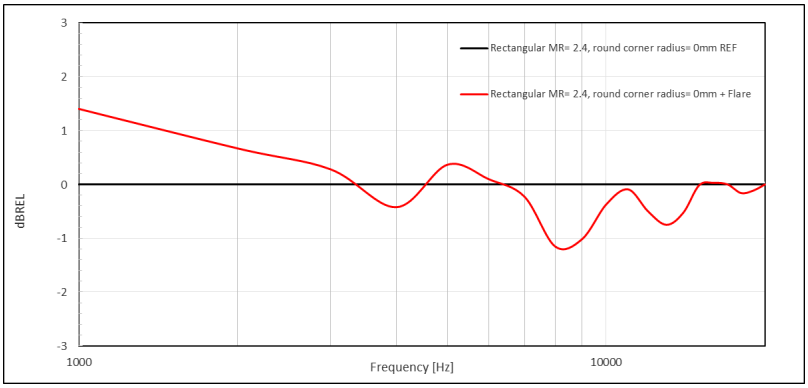

Figure 43. Normalized on axis frequency response curve of the rectangular mouth HCD exponential horn (MR= 2.4) with flared mouth (red), referenced to the same horn with unflared mouth (black).

We can deduce also that the total frequency averaged SPL contribution of a flared mouth, using the flare profile of Fig. 40, is positive for the circular, near to zero for the elliptical and negative for the rectangular mouth horn, Fig. 43.
Analyzing now the elliptical mouth exponential horn (MR= 1.7) polar patterns of Fig. 44, we can see that on the constant directivity plane A, the flared mouth has a very small influence on the off-axis horn performance, because the wave-front is guided by the pseudo-conical shape. On the plane B, showed in Fig. 45, the flared mouth has a significant influence due to acoustic pressure. As per above, for mouth ratios> 1 (in general for all horns having a different progression on perpendicular side sections) there is

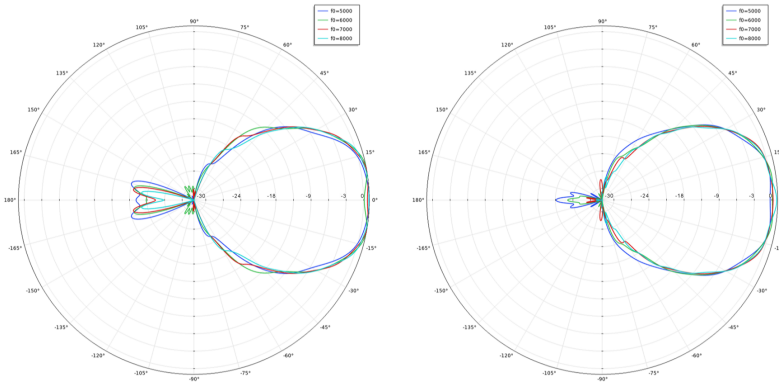

Figure 44. Elliptical mouth exponential horn (MR= 1.7) polar patterns on plane A. Unflared (left) and flared mouth (right).

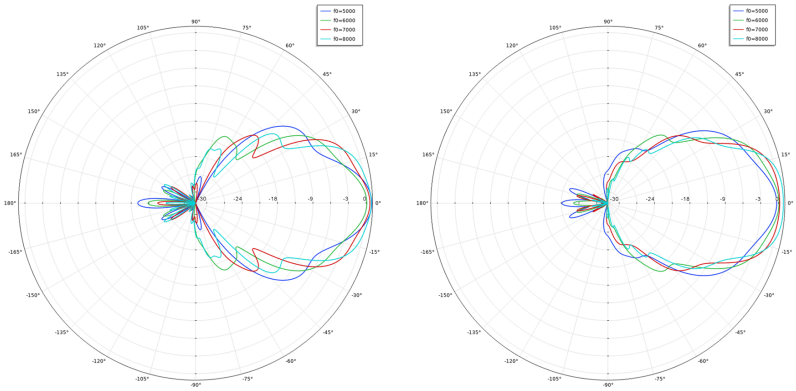

Figure 45. Elliptical mouth exponential horn (MR= 1.7) polar patterns on plane B. Unflared (left) and flared mouth (right).

not a unique profile to build a flared mouth, but we need to differentiate it along the mouth loop. Resuming, on the horn constant directivity profile we can reduce the flare dimension as it has a minor impact, on the contrary on plane B it has a great importance and it must be accounted for to obtain a good polar pattern, frequency and impulse response at the same time. The frequencies where we can find problems on directivity polar patterns depend on geometry, dimension and expansion of the horn and in this case are in the range 5÷8 kHz. Please note that the according to a polar patterns analysis for a horn application in full space (4π steradian solid angle), indeed the problems could be outside the horn coverage angle, but when we apply the horn in half space (2π steradian), meaning that horn is applied on a panel, the flared mouth could have a different result. Underlining that the flared mouth of Fig. 40 is not considered for a 4π steradian application, but it is specific for 2π steradian. In general for 2π steradian is also necessary to study the interactions between the horn mouth and other obstacles influencing directivity, frequency or impulse response, for example if the horn or the other loudspeakers are flush mounted.

9 HCD mathematical model

As we know from Beranek's [5] text, Section 11 of Chapter 5, when we have a junction of two pipes with different areas a discontinuity occurs creating a reflected wave which will be sent back toward the source. A similar behavior happens for the changes in multiflare horns [6] because of a step and/or a sharp change in the cross-sectional areas flare constant, causing a discontinuity in radiation impedance. In multiflare horns the boundaries could be very convenient for directivity control, counter side these horns type cannot always guarantee a perfect impulse response if compared to an exponential expansion. Keeping a similar concept of the radial horn [7] (two planes differentiation), HCD horn's algorithm reduces these flare changes to reach the target directivity on one plane and at the same time it preserves the loading of a designated expansion, minimizing any discontinuity in radiation impedance. The radiation impedance Z is defined as the complex ratio of the pressure to the particle velocity. The real and imaginary components of Z may be expressed as $Z = \mathrm{R} + i\mathrm{X}$, where R is the

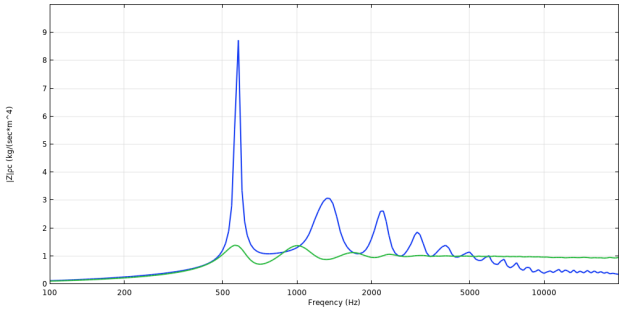

Figure 46. Normalized mouth (blue) and throat (green) radiation impedance of the flared circular exponential horn.

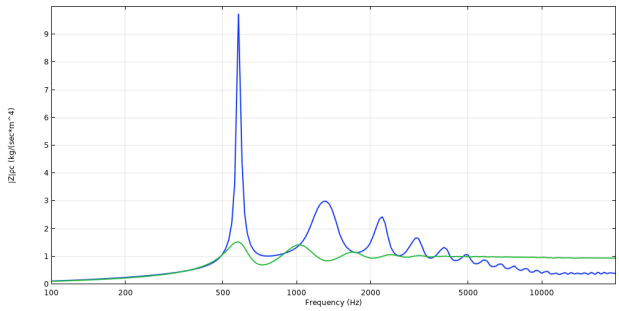

Figure 47. Normalized mouth (blue) and throat (green) radiation impedance of the flared elliptical exponential HCD horn MR= 1.7.

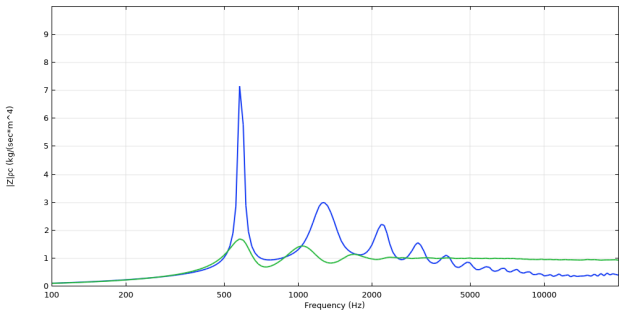

Figure 48. Normalized mouth (blue) and throat (green) radiation impedance of the flared elliptical exponential HCD horn MR= 2.4.

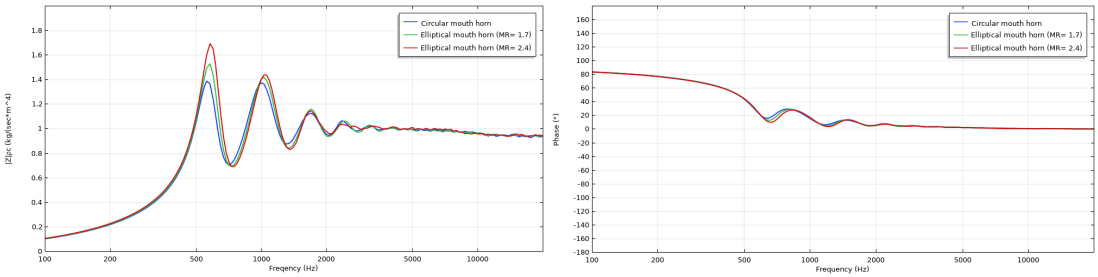

Figure 49. Throat radiation impedances comparison.

resistive and X is the reactive portion of the radiation impedance. The low frequency directivity control depends on the used expansion function and selected parameters, generally control starts from mouth Z_{min}after the frequency cut-off. HCD horn can transform all expansions, keeping an equivalent circular profile on one plane while on the perpendicular one the profile is mainly governed by the mouth ratio, having a tendency to conic if the mouth ratio$\gg$ 1. The algorithm is based on the following discretization process. In the top of Fig. 50 is shown an axisymmetric circular horn, where At is the cross-sectional area of the horn throat and Am_R is the cross-sectional area of the horn mouth,

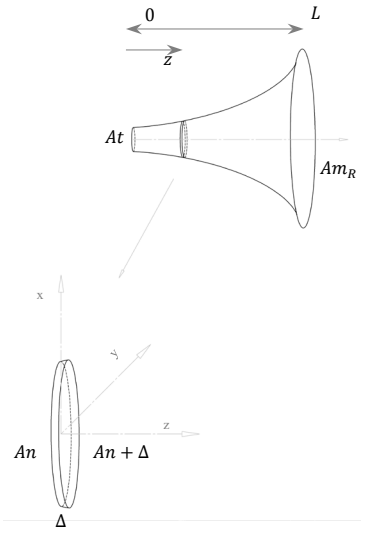

Figure 50. Axisymmetric circular horn geometry and model discretization. Variables are defined in text.

characterized by the mouth shape and its ratio. If for $R = 1$ we have a circular mouth horn, for $R > 1$ we have an elliptical mouth horn. If for $R = 1$ we have a square mouth horn, for $R > 1$ we have a rectangular mouth horn. Assuming the horn walls are rigid and the fundamental acoustic equations are applicable, the horn volume is discretized by a series of N conical waveguide elements, showed in the bottom image of Fig. 50, as a small air volume Vn_R that expands as a function of the distance k along the z axis, between 0 and the horn length L. The volume Vn_R is given by the two bounding cross-sectional areas An, $An + \Delta$ and the finite sub-interval width Δ, where Δ represents a small increment of the horn expansion. Assuming cross-sections parallel to the plane Oxy at the corresponding $z = nk$, for $0 \leq n \leq$ N all the contours are concentric circles centered at the origin and for $k \to 0$, Δ became a differential infinitesimal step dz. The expansion of a horn (exponential, tractrix, spherical…) is expressed by its function ψn and the rate expansion of ψn is the solution for finding the surface area Am_R and all An along z. Exploring the elliptical mouth case (the procedure is analogous for square and rectangular mouth cases) with a circular throat, the first condition is the equal volume arrangement:

$$Vn_{R=1} - Vn_{R>1} = 0 \tag{1}$$

where $Vn_{R=1}$ represents the small conical waveguide element with circular shape sides and $Vn_{R>1}$ represents the small conical waveguide element with elliptical shape sides, given by the shape ratio $R > 1$. The small air volume $Vn_{R>1}$ has the two sides An, $An + \Delta$ with elliptical shapes, characterized by their specific eccentricity ε_n and their linear eccentricity f_n, where ε is a non-negative real number ($0 \leq \varepsilon < 1$) and f is the distance between the ellipse center and either of its two foci.
For $\Delta \to 0$ the first condition (1) will be:

$$An_{R=1} - An_{R>1} = 0 \tag{2}$$

Where $z = kn$ and $0 \leq z \leq$ L

$$An = At \xrightarrow{yields} \varepsilon = 0 \tag{3}$$

$$An = Am_{R>1} \xrightarrow{yields} \varepsilon = \frac{f}{a} \tag{4}$$

Where a is defined as the horn mouth semi-major axis. Since ε_n represents the circular shape deviation along z axis, selecting a small finite sub-interval width Δ (in other words a small mesh) the radiation impedance is subjected to a corresponding small variation, for instance visible on radiation impedance graphs, Figs. 47, 48 compared to Fig. 46. Small differences observable in Fig. 49 are due to mouths flared end and selected sub-intervals. Considering the circular shape as a degeneration of the elliptical shape (having $a = b$ for $R = 1$, where b in the initial condition is defined as the radius of the circle and then as the elliptical horn mouth semi-minor axis, stretched by a factor R, that for $R > 1$ is always $b < a$ ($a, b > 0$ and $a, b \in \mathbb{R}$)), the conditions (3) and (4) can be expressed as a unique function depending on eccentricity $\varepsilon(z)$ where:

$$\varepsilon_{R=1}(z) = 0 \tag{5}$$

$$\varepsilon_{R>1}(0) = 0 \tag{6}$$

$$\varepsilon_{R>1}(L) = \frac{f}{a} \tag{7}$$

Defined a circular mouth horn by the expansion ψn and the rate expansion of ψn for finding the surface area An, it is possible to compute an equivalent elliptical mouth horn, defining $\varepsilon_{R>1}(z)$ that respect the conditions (6) and (7):

$$\varepsilon_{R>1}(z) = \sqrt{1 - \left(\frac{\pi \left(\sqrt{\frac{An}{\pi}} - z\delta \right)^2}{An} \right)^2} \tag{8}$$

where δ is a fixed term used for the eccentricity progression along the horn length z. Horns developed for this paper a linear function (9) along z has been used:

$$\delta = \frac{bm_{R=1} - bm_{R>1}}{L} \tag{9}$$

Some $\varepsilon_{R>1}(z)$ curves are reported in Fig. 51 for different mouth ratios, where each curve represents how fast the section transformation is for a given HCD horn mouth ratio.

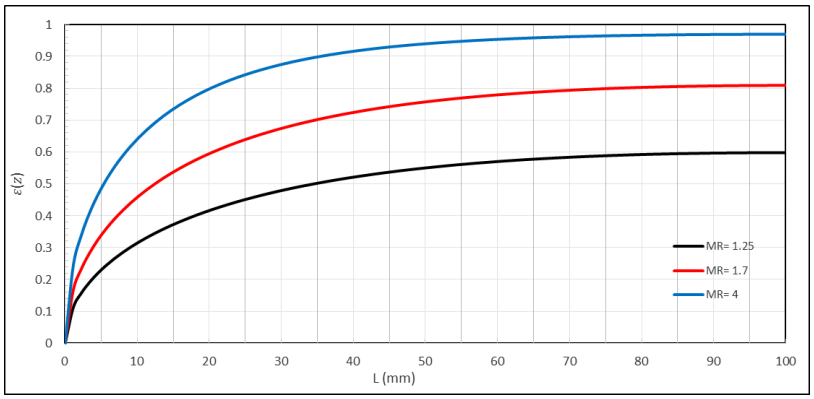

Figure 51. Eccentricity curves example for a given HCD horn with different mouth ratios.

The equation of a circle can be written in terms of x in the first quadrant:

$$y(x) = \sqrt{b^2 - x^2} \tag{10}$$

Finding the enclosed area:

$$A_{circle} = \int_{-b}^{b} 2\sqrt{b^2 - x^2}\, dx \tag{11}$$

Integrating the horn length referred to a function of z and assuming $\beta(z)$ the function of b along z:

$$Vn_{R=1} = \int_0^L A_{circle}\,(z)\, dz = \int_0^L \int_{-\beta(z)}^{\beta(z)} 2\sqrt{\beta^2(z) - x^2}\, dx\, dz \tag{12}$$

The equation of an ellipse can be written in terms of x in the first quadrant:

$$y(x) = b\sqrt{1 - \frac{x^2}{a^2}} \tag{13}$$

For $x \in [-a, a]$, $y(x)$ represents the positive half of the ellipse, so twice the integral of $y(x)$ over the same interval will be the area:

$$A_{ellipse} = \int_{-a}^{a} 2b\sqrt{1 - \frac{x^2}{a^2}}\, dx \tag{14}$$

Integrating the horn length referred to a function of z and assuming $\alpha(z)$ the function of a along z:

$$Vn_{R>1} = \int_0^L A_{ellipse}\,(z)\, dz = \int_0^L \int_{-\alpha(z)}^{\alpha(z)} 2\beta(z)\sqrt{1 - \frac{x^2}{\alpha^2(z)}}\, dx\, dz \tag{15}$$

And expressing through (8):

$$Vn_{R>1} = \int_0^L \int_{-\alpha(z)}^{\alpha(z)} 2\left(\sqrt{\frac{An}{\pi}} - z\delta \right) \sqrt{1 - \frac{x^2(1 - \varepsilon^2(z))}{\left(\sqrt{\frac{An}{\pi}} - z\delta \right)^2}}\, dx\, dz \tag{16}$$

We can write (1) in integral form as a function of An and ε:

$$\int_0^L \int_{-\beta(z)}^{\beta(z)} 2\sqrt{\frac{An}{\pi} - x^2}\, dx\, dz \; - \int_0^L \int_{-\alpha(z)}^{\alpha(z)} 2\left(\sqrt{\frac{An}{\pi}} - z\delta\right) \sqrt{1 - \frac{x^2(1-\varepsilon^2(z))}{\left(\sqrt{\frac{An}{\pi}} - z\delta\right)^2}}\, dx\, dz = 0 \tag{17}$$

Starting by the known surface area, satisfying the boundary conditions (1), (3) and (4), solving them in a system (17) in function of the eccentricity (8), the result is an elliptical HCD horn. Using an analogous procedure with a radius, instead eccentricity, as the degenerate function in the second term of (17), it is possible to find an equivalent expression for calculating the square mouth horn. For the rectangular mouth horn is also necessary to add the major axis in the degenerate function of the square mouth, using this new variable as a divergence function between b and a along the horn length L. More generally it's possible to produce a HCD horn starting from any known (or a new) expansion function, using one or more degenerate functions to adapt throat to mouth profiles along the horn length, keeping the correspondence between volumes.

10 Conclusions

A new family of horns has been presented, the Hybrid Constant Directivity (HCD). Horn-driver simulations are conducted using a method already presented from the author and a further development about the main limit is disclosed here. A new model is proposed, leading to obtain a frequency band average SPL difference of about ±1.5 dB between horn-driver measurement and FEA simulation. The new model is then used for simulating horns directivity and beam-width. A horn expansions efficiency analysis is given, through the SPL comparison among exponential, tractrix and spherical horns. A discussion about a flare side section differentiation for horns having mouth ratios> 1 is disclosed, more generally with a different progression on perpendicular side sections. Finally, the mathematical model for calculating HCD horns is presented. It is shown how the HCD horn's algorithm reduces flare variations to reach the target directivity on one plane and at the same time how it preserves the designated expansion loading, minimizing any discontinuity in HCD radiation impedance. Overall it is exposed how it is possible to produce an HCD horn starting from any known (or a new) expansion function, using one or more degenerate functions to adapt throat to mouth profiles along the horn length, keeping the correspondence between volumes.

Last, I would like to thank my great friend Mauro De Carolis for fruitful opinions exchange about critical aspects of software development.

References

[1] D. Cinanni, *Simulation of Horn Driver Response by Direct Combination of Compression Driver Frequency Response and Horn FEA*, Presented at the Comsol Conference in Grenoble, 2015.

[2] *SpeakerLAB Horn.ell.a* datasheet.

[3] Bob H. Smith, *An Investigation of the Air Chamber of Horn Type Loudspeakers*, The Journal of the Acoustical Society of America, Vol.25 No.2, pp. 305-312, 1953.

[4] M. Dodd and J. Oclee-Brown, *A New Methodology for the Acoustic Design of Compression Driver Phase Plugs with Concentric Annular Channels*, Presented at the 123rd AES Convention, 2007.

[5] L. L. Beranek, *Acoustics*, Acoustical Society of America, Woodbury, NY, Revised Edition 1993.

[6] C. A. Henricksen, M. S. Ureda, *The Manta-Ray Horns*, Presented at the 58th AES Convention, 1977.

[7] D. B. Keele Jr., *What's so sacred about exponential horns?*, Presented at the 51st AES Convention, 1975.